NEURO

Comparison of 3D multi-echo gradient-echo and 2D T2* MR sequences for the detection of arterial thrombus in patients with acute stroke

Jérôme Hodel · Xavier Leclerc · Wassef Khaled · Ruben Tamazyan ·
Mathieu Rodallec · Sophie Gerber · Raphael Blanc · Mohamed Benadjaoud ·
Oriane Lambert · Cécile Rabrait · Mathieu Zuber · Alain Rahmouni · Marc Zins

Abstract

Objectives We compared a multi-echo gradient-echo magnetic resonance sequence (susceptibility-weighted angiography [SWAN]) with the T2* sequence for the detection of an arterial thrombus in acute ischaemic stroke.

Methods Seventy-four consecutive patients with acute ischaemic stroke were included. Proximal arterial occlusions were diagnosed using time-of-flight (TOF) magnetic resonance angiography (MRA). Two-dimensional (2D) axial reformats from 3D SWAN were generated to match with 2D T2* images. For arterial thrombus detection, each set of MR images (T2*, 2D SWAN reformats and 3D multiplanar SWAN images) was examined independently and separately by three observers who assigned the images to one of three categories: (0) absence of thrombus, (1) uncertain thrombus, (2) certain thrombus. Agreement and diagnostic accuracy were calculated.

Results Twenty-four proximal arterial occlusions involving the anterior (n=20) or posterior (n=4) circulation were found. Inter-observer agreement was moderate using T2* images (κ=0.58), good using 2D SWAN reformats (κ=0.83) and excellent using multiplanar SWAN images (κ=0.90). For the diagnosis of thrombus, T2* images were 54 % sensitive and 86 % specific, 2D SWAN reformats were 83 % sensitive and 94 % specific and SWAN multiplanar analysis was 96 % sensitive and 100 % specific.

Conclusions Three-dimensional SWAN sequence improves the detection of arterial thrombus in patients with acute ischaemic stroke in comparison with the 2D T2* sequence.

Key Points

• *Multi-echo gradient-echo MR (e.g. susceptibility-weighted angiograph, [SWAN]) is increasingly used in neuroradiology.*

• *Compared with conventional T2* sequences, SWAN improves detection of arterial thrombus.*

• *Multiplanar SWAN analysis had the best diagnostic performance for arterial thrombus detection.*

• *Sensitivity was 96 % and specificity 100 %.*

• *Findings support combination of time-of-flight and susceptibility effects in suspected acute stroke.*

Keywords Acute ischaemic stroke · Arterial thrombus · Susceptibility-weighted imaging · T2* sequence · Time of flight magnetic resonance angiography

J. Hodel (✉) · W. Khaled · M. Rodallec · S. Gerber · M. Zins
Department of Radiology, Hôpital Saint Joseph, 186, rue Raymond
Losserand, Paris, France
e-mail: jerome.hodel@gmail.com

J. Hodel · X. Leclerc
Department of Neuroradiology, CHRU Roger Salengro, Lille, France

R. Blanc · O. Lambert
Department of Neuroradiology, Fondation Ophtalmologique
Rothschild, Paris, France

M. Benadjaoud
Inserm, CESP Centre for Research in Epidemiology and Population
Health, U1018, Radiation Epidemiology Team,
Villejuif, France

C. Rabrait
GE Healthcare, Clinical Science Development Group, Buc, France

R. Tamazyan · M. Zuber
Department of Neurology, Hôpital Saint Joseph, Paris, France

A. Rahmouni
Department of Radiology, Hôpital Henri Mondor, Créteil, France

Abbreviations and acronyms

SWI	Susceptibility-weighted imaging
TOF MRA	Time-of-flight magnetic resonance angiography
SWAN	Susceptibility-weighted angiography
GRE	Gradient echo
ACA	Anterior cerebral artery
PCA	Posterior cerebral artery
MCA	Middle cerebral artery
FLAIR	Fluid-attenuated inversion recovery

Introduction

In patients with acute stroke, the exact location of the thrombus must be indicated, especially when a thrombolytic therapy is considered [1–4]. While magnetic resonance imaging (MRI) protocols may vary among institutions, the gradient-echo (GRE) T2* sequence is widely used in clinical routine to rule out brain haemorrhage and to detect arterial thrombus. Using T2* images, arterial thrombus usually appears as a signal loss along the course of an artery, a finding commonly called the "susceptibility sign", initially described in patients with occlusion of the middle cerebral artery (MCA) [5–7]. These susceptibility changes are attributed to the high deoxyhaemoglobin content and retraction of fresh thrombus [8–10].

Susceptibility-weighted MR sequences provide additional information about acute stroke [11–13] or brain vascular malformations [14]. Susceptibility-weighted imaging (SWI) is a single echo MR sequence that combines phase and magnitude signal for the visualisation of brain veins [15–17]. In this study, we evaluated a 3D multi-echo gradient-echo (GRE) MR sequence called "SWAN" (susceptibility-weighted angiography) that uses the sole magnitude signal [18, 19]. Using this sequence, 12 echoes are acquired with a time echo (TE) ranging from 15 to 35 ms. Shorter echoes lead to time-of-flight (TOF) in-flow effect, visible within the brain arteries, whereas longer echoes are sensitive to the susceptibility effects commonly observed within brain veins or haemoglobin products. Therefore, using SWAN, it is possible to simultaneously evaluate brain arteries and veins [18, 20]. These technical aspects also suggest that SWAN could be more accurate for the detection of arterial thrombus compared with the conventional T2* sequence because of the improved contrast between the arterial TOF effect and the thrombus-related susceptibility effect.

To our knowledge, no data are available on the diagnostic performance of SWAN in patients presenting with acute arterial thrombus. In this study, our objective was to compare the SWAN and the conventional T2* MR sequences for the detection of arterial thrombus in patients with acute ischaemic stroke.

Materials and methods

Patients

This study was approved by our institutional review board and written informed consent was obtained from all subjects. For this prospective study, patient inclusion criteria were as follows:

1. Patients explored at 1.5- or 3-T MRI
2. Time window between symptom onset and brain imaging less than 24 h
3. Absence of brain haemorrhage
4. Presence of acute ischaemic lesion on diffusion-weighted (DW) images
5. Absence of gadolinium administration

From October 2012 to February 2013, 124 consecutive patients were explored using MRI for a suspected acute stroke. Of these 124 patients, 17 presented with haemorrhage and MR images were not assessable in nine because of motion artefacts. Among the remaining 98 patients, 74 (31 men, 43 women; mean age 74 years, minimum 35 years, maximum 92 years) presented acute ischaemic lesion on DW imaging and were included in the study. All these patients underwent imaging with both the T2* and SWAN MR sequences (35 at 1.5 T, 39 at 3 T).

Mean National Institutes of Health Stroke Scale (NIHSS) at admission was 9 (minimum = 1, maximum = 23). The 74 patients presented 83 acute ischaemic lesions on DW images involving middle cerebral artery (MCA) territory ($n = 46$), anterior cerebral artery (ACA) territory ($n = 6$), vertebro-basilar artery territory ($n = 17$) or watershed territory ($n = 14$). Thirteen patients were treated by rtPA, one by stenting and two by mechanical thrombectomy.

Image acquisition

MRI examinations were performed at 1.5 T (MR450W; GE Healthcare, Milwaukee, USA) in 35 patients and at 3-T MRI (Discovery MR750; GE Healthcare) for 39 patients using 8- and 12-channel array head coils respectively. All patients who met the inclusion criteria were investigated with the 3D SWAN sequence in addition to the routine MR protocol, which includes DW, GRE T2*, 2D FLAIR and TOF MRA sequences. The total MRI protocol duration was 13 min. 3D SWAN source images were reformatted into 5-mm-thick axial sections to match the section thickness and the acquisition plane of the 2D T2* images. The parameters for T2* and SWAN sequences at 1.5 and 3 T are summarised in Table 1.

Table 1 Imaging parameters of T2* and susceptibility-weighted angiography (SWAN) at 1.5 and 3 T

Parameter	T2*	SWAN	T2*	SWAN
MRI field strength	1.5 T	1.5 T	3 T	3 T
Acquisition plane	Axial	Axial	Axial	Axial
TR (ms)	720	76	740	40
TE (ms)	23	48 [a]	18	25 [a]
Matrix size	256×224	256×224	256×224	256×224
Field of view (mm)	240×180	240×180	240×180	240×180
Slice thickness (mm)	5	2 (2D reformat: 5)	5	2 (2D reformat: 5)
Coverage (mm)	150	100	150	100
No. of slices	30	50	30	50
Acquisition time	2 min 50 s	2 min 50 s	2 min 50s	2 min 43 s

TR repetition time, *TE* echo time, *No. of slices* number of slices acquired, *2D reformat* 5-mm-thick axial reformatted views of the 3D SWAN sequence (leading to the same voxel size when compared with the T2* sequence)

[a] Effective TE (using the SWAN sequence, 12 echoes are acquired with a TE ranging from 15 to 35 ms. Indeed the single echo time provided in the method section is an effective TE)

Image analysis

Image quality and diagnosis of proximal arterial occlusion

In this study, the reference standard for the diagnosis of arterial occlusion was based on TOF MRA. Three experienced neuroradiologists (S.G., M.R. and J.H.), with 20, 16 and 11 years' experience respectively, evaluated the TOF images for each patient in consensus. Multiplanar analysis, including thin oblique MIP reformatted views, was available for this statement. The number and location of the proximal arterial occlusions, involving vertebro-basilar arteries, M1M2, P1P2 or A1A2 arterial segments, were assessed by the three neuroradiologists using the TOF MRA.

Artefacts within the SWAN and T2* images were also graded according to a three-point scale (0, no artefacts; 1, artefacts that did not impair image analysis; 2, artefacts that impaired image analysis).

Comparison between T2 and SWAN MR sequences*

Three additional readers (W.K., R.B. and R.T.), with 7, 16 and 9 years' experience respectively, independently and separately analysed in a randomised order the SWAN and T2* images of each patient on a PACS workstation. The readers assessed three sets of images separately in a randomised order: (1) 2D T2* images, (2) 5-mm-thick axial reformations from 3D SWAN sequence and (3) multiplanar analysis of the SWAN sequence with thin sections and minimal/maximal intensity projection (MinIP and MIP respectively) reformations in arbitrary planes. The three independent blinded lectures took place 4 weeks apart to avoid recall bias. Only the T2* and SWAN images were available, the readers were blinded to clinical data and blinded to other MR sequences.

For each patient and each set of images, the readers were asked to assess the presence or absence of an arterial thrombus, defined as a focal susceptibility effect within vertebro-basilar arteries, M1M2, P1P2 or A1A2 arterial segments. Following these guidelines, image sets were graded according to the following three-point scale: (0) absence of thrombus (no susceptibility effect), (1) uncertain thrombus (uncertain signal loss within brain arteries) and (2) certain thrombus (strong susceptibility effect within brain arteries with accurate localisation and delineation of the thrombus). Disagreements between the three blinded readers were resolved in consensus reading.

Statistical analysis

Statistical analyses were performed using SAS software version 9.3 (SAS Institute, Cary, NC, USA).

We used the generalised kappa (κ) of Fleiss as a measurement of agreement among the three blinded readers. The kappa statistics were calculated using the *AgreeStat_3SAS* SAS macro and interpreted as follows: less than 0.00, poor agreement; 0.00–0.20, slight agreement; 0.21–0.40, fair agreement; 0.41–0.60, moderate agreement, 0.61–0.80, substantial agreement; 0.81–1.00, almost perfect agreement. The statistical significance of differences between kappa values was calculated using a bootstrap method for comparison of correlated κ coefficients.

In order to calculate the inter-technique agreement, the diagnosis of thrombus was made in two different steps. The first step consisted to interpret each set of images separately by the readers blinded from MRA findings. The second step consisted to interpret the discrepancies in consensus by the three readers together. In this step, all uncertain diagnoses were classified as 0, (absence of thrombus) or 1

(presence of a thrombus). The sensitivity, specificity, positive predictive value, negative predictive value and their exact confidence interval where calculated using PROC FREQ (BINOMIAL option in the EXACT statement). The level of statistical significance was $P < 0.05$.

Results

Patients

TOF MRA was available for the 74 patients included. Twenty-four arterial occlusions, involving the anterior ($n = 20$) or the posterior ($n = 4$) circulation, were identified in 24 patients. The 24 arterial occlusions involved the M1M2 ($n = 19$), A2 ($n = 1$), P2 ($n = 2$), V4 ($n = 2$) arterial segments.

Image quality

Using the SWAN sequence, the brain arteries appeared hyperintense owing to the TOF effect, whereas an intermediate signal was noted on the T2* images. Susceptibility artefacts were observed in all patients at the air–bone interfaces in both T2* and SWAN images. These artefacts were mainly located at the skull base and near the paranasal sinuses. In T2* images, such susceptibility artefacts affected the visualisation of the basilar artery for all the patients (rated 2), whereas a continuous TOF effect was still visible for all patients using the SWAN sequence (rated 1).

Inter-observer agreement

Results are summarised in Table 2.

There was a disagreement between the three blinded readers (i.e. at least one score different) for 17 patients using the T2* images (7 at 1.5 T and 10 at 3 T), for 8 patients using the 2D reformatted view of SWAN images (5 at 1.5 T and 3 at 3 T) and for 4 patients using the 3D SWAN images (3 at 1.5 T and 1 at 3 T). For all these patients, the disagreements of image interpretation between T2* and SWAN sequences were reviewed to reach a consensus.

Table 2 Agreement among the three blinded readers for T2* images, 2D SWAN reformats and SWAN multiplanar images

	T2* images	2D SWAN reformat	SWAN MPR
All patients (n=74)			
Kappa	0.58	0.83	0.90
P value	<0.001	<0.001	<0.001
$CI_{95\%}$	0.43-0.70	0.73-0.92	0.81-0.98
1.5 T (n=35)			
Kappa	0.65	0.81	0.89
P value	<0.001	<0.001	<0.001
$CI_{95\%}$	0.47-0.82	0.68-0.95	0.75-1
3 T (n=39)			
Kappa	0.51	0.85	0.89
P value	<0.001	<0.001	<0.001
$CI_{95\%}$	0.29-0.69	0.69-1	0.72-1

Table 3 Accuracy of T2* and SWAN MR sequences for the diagnosis of arterial thrombus in patients with suspected acute ischaemic stroke

	T2* images	2D SWAN reformat	SWAN MPR
Blinded evaluation			
Rated 0	167	160	155
Rated 1	41	11	6
Rated 2	14	51	61
Diagnosis of thrombus			
All patients (n=74)			
TN	43	47	50
TP	13	20	23
FN	11	4	1
FP	7	3	0
Sensitivity, $CI_{95\%}$	0.54 (0.33-0.74)	0.83 (0.63-0.95)	0.96 (0.79-1)
Specificity, $CI_{95\%}$	0.86 (0.73-0.94)	0.94 (0.83-0.99)	1 (0.93-1)
PPV, $CI_{95\%}$	0.65 (0.41-0.85)	0.87 (0.66-0.97)	1 (0.85-1)
NPV, $CI_{95\%}$	0.80 (0.66-0.89)	0.92 (0.81-0.98)	0.98 (0.90-1)
1.5 T (n=35)			
TN	17	19	20
TP	8	12	15
FN	7	3	0
FP	3	1	0
Sensitivity, $CI_{95\%}$	0.53 (0.27-0.79)	0.80 (0.52-0.96)	1 (0.78-1)
Specificity, $CI_{95\%}$	0.85 (0.62-0.97)	0.95 (0.75-1)	1 (0.83-1)
PPV, $CI_{95\%}$	0.73 (0.39-0.94)	0.92 (0.64-1)	1 (0.78-1)
NPV, $CI_{95\%}$	0.71 (0.49-0.87)	0.90 (0.65-0.97)	1 (0.83-1)
3 T (n=39)			
TN	26	28	30
TP	5	8	8
FN	4	1	1
FP	4	2	0
Sensitivity, $CI_{95\%}$	0.56 (0.21-0.86)	0.89 (0.52-1)	0.89 (0.52-1)
Specificity, $CI_{95\%}$	0.87 (0.70-0.96)	0.93 (0.78-0.99)	1 (0.88-0.96)
PPV, $CI_{95\%}$	0.56 (0.21-0.86)	0.80 (0.44-0.98)	1 (0.63-1)
NPV, $CI_{95\%}$	0.87 (0.69-0.96)	0.97 (0.82-1)	0.97 (0.83-1)

2D SWAN reformat: 2D 5 mm-thick reformatted views of the SWAN sequence, *SWAN MPR*: multiplanar images of the SWAN sequence, *Blinded Evaluation*: rating (0, 1 or 2) for all patients by the three blinded readers for each approach (T2*, 2D SWAN reformat or multiplanar SWAN images), *Diagnosis of thrombus*: number of arterial thrombus detected for each approach and accuracy parameters based on the consensus of the three blinded readers; *TN*: true negatives, *TP*: true positives, *FN*: false negatives, *FP*: false positives, *PPV*: positive predictive value, *NPV*: negative predictive value

Considering the whole cohort (1.5 and 3 T), the agreement between readers was significantly higher when using 2D reformats or multiplanar SWAN images (almost perfect) in comparison with the T2* images (moderate agreement; $P = 0.005$ and <0.001 respectively). There was no significant difference between 2D reformats and multiplanar SWAN images ($P = 0.20$).

In patients explored at 1.5 T, the agreement was significantly improved using multiplanar SWAN images compared with T2* images ($P = 0.023$). There was no significant difference between 2D reformats and T2* images ($P = 0.15$) and between 2D reformats and multiplanar SWAN images ($P = 0.44$).

In patients explored at 3 T, the agreement between readers was significantly higher when using 2D reformats or multiplanar SWAN in comparison with the T2* images ($P = 0.016$ and 0.006 respectively). There was no significant difference between 2D reformats and multiplanar SWAN images ($P = 0.31$).

Comparison between T2* and SWAN MR sequences

Results are summarised in Table 3.

Based on the blinded lecture of the three readers, the diagnosis of thrombus remained "uncertain" (rated 1) for 18.5 % of the assessments using T2* images, while the rate of "uncertain" diagnosis was 5 % using the 2D reformats of SWAN and only 2.7 % using SWAN multiplanar images.

All the diagnostic accuracy parameters were improved using SWAN images in comparison to T2* images.

Examples of improved thrombus detection using SWAN are given in Figs. 1, 2 and 3.

Discussion

The demonstration of arterial occlusion may have prognostic and therapeutic implications in acute stroke patients. Detection of arterial thrombus was significantly improved with the SWAN

Fig. 1 T2* (**a**) and susceptibility-weighted angiography (SWAN) (**b-d**) images of patient 14 with acute ischaemic stroke in the left middle cerebra artery (MCA) territory due to a left M2 occlusion. The arterial thrombus was missed (rated 0) by the three blinded readers using the T2* images (**a**, *arrow*). Using the 5-mm-thick axial reformatted views of SWAN, the thrombus was correctly identified (**b**, *arrowhead*) by all the readers as "certain" (rated 2). Note that SWAN axial oblique thinner slices (**c**, *arrowhead*) and MinIP reformations (**d**, *arrowhead*) further improved the thrombus delineation
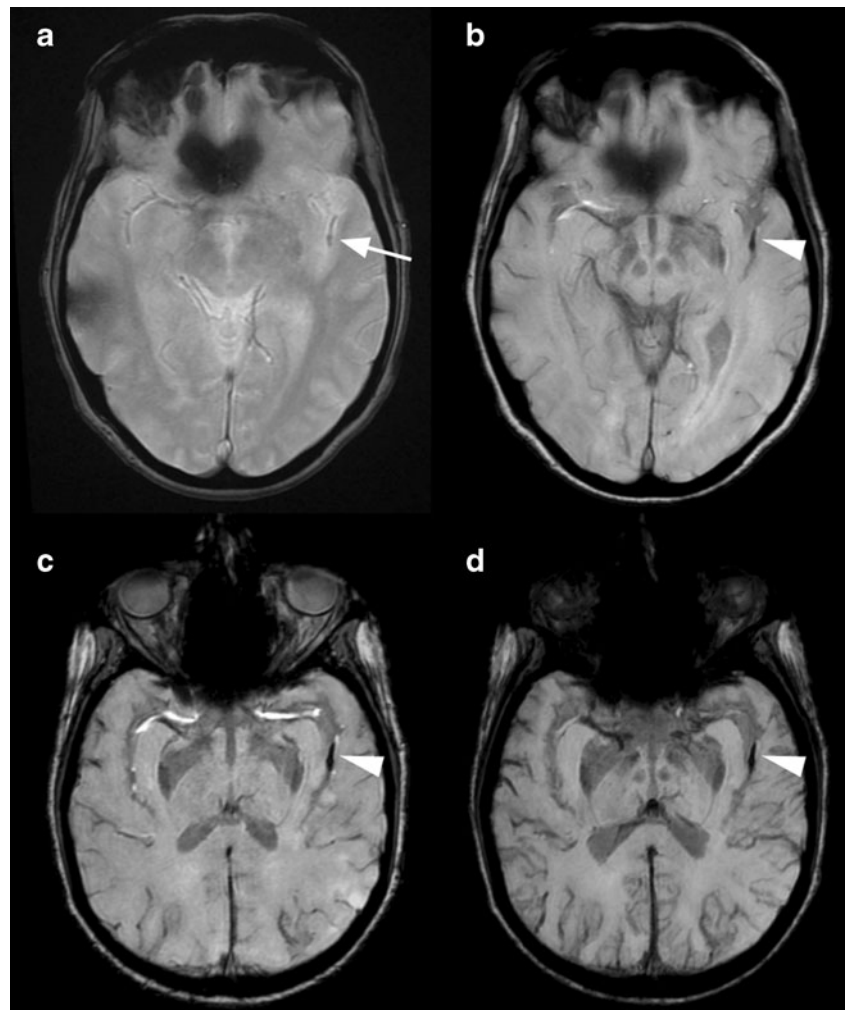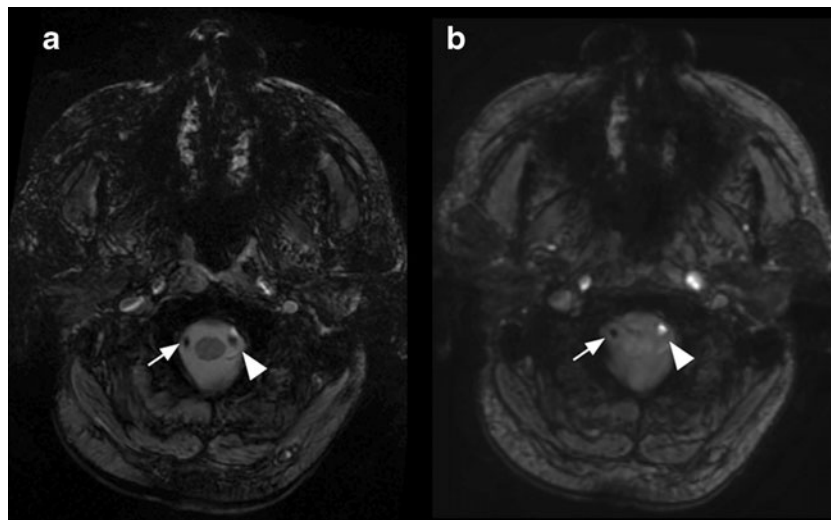
Fig. 2 T2*(**a**) and SWAN (**b**) images of patient 39 with acute ischaemic stroke in the right posterior inferior cerebellar artery (PICA) territory due to an occlusion of the right V4 segment. An arterial occlusion involving the right V4 arterial segment was identified using the time of flight magnetic resonance angiography (TOF MRA). The arterial thrombus was missed (rated 0) by the three blinded readers using T2* images (**a**, *arrow*). Indeed, there was no evident signal difference between the two vertebral arteries (**a**, *arrow* and *arrowhead*) using this sequence. On the other hand, using SWAN images, the thrombus was easily identified (**b**, *arrow*) owing to the signal contrast between the hypointensity of the arterial thrombus, related to a susceptibility effect (**b**, *arrow*), and the hyperintensity of the contralateral left V4 segment, due to a blood inflow effect (TOF effect) (**b**, *arrowhead*)

sequence in comparison with the conventional T2* sequence. This finding strongly supports the use of a multi-echo gradient-echo MR sequence combining TOF and susceptibility effects, such as SWAN, rather than the T2* sequence in patients with suspected acute ischaemic stroke.

Previous studies suggested the added value of SWI or SWAN in comparison with the conventional 2D T2* sequence for the diagnosis of intracranial hemorrhagic lesions [21, 22] or cavernous malformations [23]. This study represents the largest to date that compares the 3D SWAN and T2* MR sequences for the detection of arterial thrombus. Susceptibility-weighted angiography is a 3D multi-echo GRE MR sequence that differs

from the SWI sequence [19]. Using SWAN, shorter echoes (acquired with TE between 15 and 25 ms) provide information about blood inflow effects (TOF effect), highlighted by MIP reformations, whereas longer echoes (acquired with TE between 25 and 35 ms) are more sensitive to susceptibility effects, better demonstrated with MinIP reformations [18, 24]. The echo combination technique used is an echo-selective "sum-of-squares" combination that improves the signal to noise ratio in comparison with a single echo method such as SWI [19].

To improve the comparison between the 2D T2* and the 3D SWAN MR sequences, we first used 5-mm-thick axial reformations from the 3D SWAN sequence, leading to the
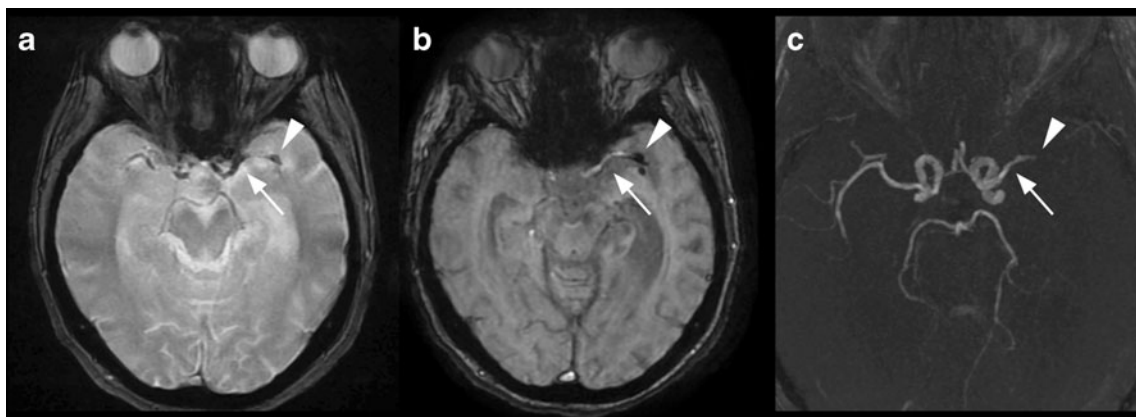

Fig. 3 T2* (**a**), SWAN (**b**) and TOF MRA (**c**) images of patient 72 with acute ischaemic stroke in the left MCA territory due to a left M2 occlusion. Using the T2* images, an arterial thrombus involving the left M2 segment (**a**, *arrowhead*) was diagnosed (rated 2) by the three blinded readers. However, an additional thrombus of the left M1 segment was suspected considering the strong hypointensity visible on T2* images (**a**, *arrow*). Using the SWAN images, the readers correctly delineated the left M2 thrombus thanks to the strong contrast between the TOF effect within the left M1 segment (**b**, *arrow*) and the susceptibility effect within the left M2 segment (**b**, *arrowhead*). The TOF MRA previously demonstrated the permeability of the left M1 segment (**c**, *arrow*) as well as the arterial occlusion located within the left M2 segment (**c**, *arrowhead*)

same voxel size compared with the T2* sequence. This approach confirmed that the diagnostic performance of the SWAN sequence was superior to that of the conventional T2*. Detection of arterial thrombus was improved with SWAN owing to the high signal contrast between the hyperintense inflow effect within arteries and the hypointense susceptibility effect of the thrombus. This finding suggests that multi-echo SWAN images are particularly well suited to the detection of arterial thrombus in patients with acute stroke. The strong agreement between readers further suggested the greater robustness of this approach. On the other hand, single echo-based techniques may decrease the diagnostic performance for the diagnosis of a thrombus owing to the hypointensity observed within brain arteries. Further studies comparing the accuracy of several commercially available susceptibility-weighted MR sequences will be needed in patients with stroke to confirm the exact role of 3D multi-echo GRE images in clinical routine.

Multiplanar analysis of the 3D SWAN images further improved the detection of arterial thrombus. There are several potential advantages of using thinner 3D slices. First, the decrease in slice thickness (i.e. the reduction of the partial volume effect) is theoretically associated with increased lesion detection. Second, 3D images can be easily co-registered with other 3D sequences. Because of the design of the SWAN sequence, gadolinium administration increases brain vein signal, resulting in a loss of the distinctive signal intensity pattern between veins and arteries. This explains why the SWAN sequence was systematically performed without gadolinium administration. Several parameters may also influence the signal of the thrombus such as deoxyhaemoglobin concentration, red blood cell integrity or thrombus structure (including fibrin and serum contents) [10, 25–28]. In the present study, all the patients underwent imaging at the acute stage (i.e. within the 24 h following onset).

Imaging of arterial occlusion with TOF MRA and visualisation of the thrombus itself using SWAN rely on two different diagnostic approaches. In the clinical practice, a fast and reliable detection of the arterial thrombus as a susceptibility artefact on SWAN images may increase diagnostic confidence particularly when a thrombolysis is considered. This may also guide the radiologist in his multiplanar analysis of TOF MRA that may be time-consuming, particularly for the diagnosis of distal occlusion. The present study was not designed to evaluate the potential of SWAN to demonstrate thrombus properties. Further studies may focus on the estimation of thrombus composition, using SWI, which may have therapeutic implications.

Our study has several limitations. First, we included 35 patients explored at 1.5 T and 39 explored at 3 T, using TOF MRA as the reference standard for the diagnosis of arterial occlusion. It is well known that TOF is improved at higher field strength, particularly for the detection of distal occlusions. As we focused our study on proximal arterial occlusions, such differences may not have significantly influenced our results. Indeed, we were able to demonstrate significant differences between SWAN and T2* for the detection of thrombus and the diagnostic accuracy parameters of the two sequences appeared similar when considering each cohort of patients explored at 1.5 and 3 T. Second, in order to reduce imaging time, contrast-enhanced MRA is not usually performed in our institution when thrombolysis is considered. This explains why we did not attempt to measure the thrombus length, even if the SWAN sequence allowed for a drastic improvement of thrombus delineation. Further studies including patients explored with computed tomography (CT) or MR post-contrast angiography are required to assess the value of SWI techniques for the detection of distal thrombus and the measurement of thrombus length. Third to improve the comparison between the 2D and 3D sequences, we modified the SWAN parameters to get similar in-plane resolution and acquisition time (i.e. 2 min 50 s). We also used parallel imaging with SWAN, ASSET with acceleration factor of 2, to further decrease the acquisition time. This explains why, in the present study, the SWAN sequence covered the brain arteries (leading to brain coverage of 10 cm for all the patients), while the T2* sequence covered the whole brain. In order to cover the whole brain, the acquisition time of SWAN would have been about 4 min. However, this slightly longer acquisition time with SWAN should be tempered considering the additional information provided on thrombus detection or blood flow dynamics [20].

Detection of arterial thrombus was improved using susceptibility-weighted angiography in comparison with the conventional T2* sequences. Such a finding strongly supports the use of a multi-echo gradient-echo MR sequence in patients with suspected acute ischaemic stroke.

References

1. Derex L, Nighoghossian N, Hermier M et al (2002) Early detection of cerebral arterial occlusion on magnetic resonance angiography: predictive value of the baseline NIHSS score and impact on neurological outcome. Cerebrovasc Dis 13:225–229

2. Hermier M, Nighoghossian N (2004) Contribution of susceptibility-weighted imaging to acute stroke assessment. Stroke 35:1989–1994

3. Schellinger PD, Fiebach JB, Hacke W (2003) Imaging-based decision making in thrombolytic therapy for ischaemic stroke: present status. Stroke 34:575–583

4. Saqqur M, Uchino K, Demchuk AM et al (2007) Site of arterial occlusion identified by transcranial Doppler predicts the response to intravenous thrombolysis for stroke. Stroke 38:948–954

5. Flacke S, Urbach H, Keller E et al (2000) Middle cerebral artery (MCA) susceptibility sign at susceptibility-based perfusion MR

imaging: clinical importance and comparison with hyperdense MCA sign at CT. Radiology 215:476–482

6. Chalela JA, Haymore JB, Ezzeddine MA et al (2002) The hypointense MCA sign. Neurology 58:1470

7. Rovira A, Orellana P, Alvarez-Sabin J et al (2004) Hyperacute ischaemic stroke: Middle cerebral artery susceptibility sign at echo-planar gradient-echo MR imaging. Radiology 232:466–473

8. Assouline E, Benziane K, Reizine D et al (2005) Intra-arterial thrombus visualized on T2* gradient echo imaging in acute ischaemic stroke. Cerebrovasc Dis 20:6–11

9. Atlas SW, Mark AS, Grossman RI et al (1988) Intracranial haemorrhage: gradient-echo MR imaging at 1.5 T. Comparison with spin-echo imaging and clinical applications. Radiology 168:803–807

10. Clark RA, Watanabe AT, Bradley WG Jr et al (1990) Acute hematomas: effects of deoxygenation, hematocrit, and fibrin-clot formation and retraction on T2 shortening. Radiology 175:201–206

11. Linfante I, Llinas RH, Caplan LR et al (1999) MRI features of intracerebral haemorrhage within 2 hours from symptom onset. Stroke 30:2263–2267

12. Patel MR, Edelman RR, Warach S (1996) Detection of hyperacute primary intraparenchymal haemorrhage by magnetic resonance imaging. Stroke 27:2321–2324

13. Schellinger PD, Jansen O, Fiebach JB et al (1999) A standardized MRI stroke protocol: comparison with CT in hyperacute intracerebral haemorrhage. Stroke 30:765–768

14. Jagadeesan BD, Delgado Almandoz JE et al (2011) Accuracy of susceptibility-weighted imaging for the detection of arteriovenous shunting in vascular malformations of the brain. Stroke 42:87–92

15. Haacke EM, Mittal S, Wu Z et al (2009) Susceptibility-weighted imaging: technical aspects and clinical applications, part 1. AJNR Am J Neuroradiol 30:19–30

16. Reichenbach JR, Venkatesan R, Schillinger DJ et al (1997) Small vessels in the human brain: MR venography with deoxyhaemoglobin as an intrinsic contrast agent. Radiology 204:272–277

17. Haacke EM, Xu Y, Cheng YC et al (2004) Susceptibility weighted imaging (SWI). Magn Reson Med 52:612–618

18. Boeckh-Behrens T, Lutz J, Lummel N et al (2012) Susceptibility-weighted angiography (SWAN) of cerebral veins and arteries compared to TOF-MRA. Eur J Radiol 81:1238–1245

19. Annamraju RB VR, Vu AT (2008) T2* weighted angiography (SWAN): T2* weighted non-contrast imaging with multi-echo acquisition and reconstruction. Proceedings of the ESMRMB, Valencia, October 2–4, Abstract 482

20. Hodel J, Blanc R, Rodallec M et al (2013) Susceptibility-weighted angiography for the detection of high-flow intracranial vascular lesions: preliminary study. Eur Radiol 23:1122–1130

21. Hayashida Y, Kakeda S, Hiai Y et al. (2013) Diagnosis of intracranial hemorrhagic lesions: comparison between 3D-SWAN (3D T2*-weighted imaging with multi-echo acquisition) and 2D-T2*-weighted imaging. Acta Radiol [Epub ahead of print]

22. Mori N, Miki Y, Kikuta K et al (2008) Microbleeds in moyamoya disease: susceptibility-weighted imaging versus T2*-weighted imaging at 3 Tesla. Invest Radiol 43:574–579

23. de Souza JM, Domingues RC, Cruz LC Jr et al (2008) Susceptibility-weighted imaging for the evaluation of patients with familial cerebral cavernous malformations: a comparison with t2-weighted fast spin-echo and gradient-echo sequences. AJNR Am J Neuroradiol 29:154–158

24. Du YP, Jin Z, Hu Y, Tanabe J (2009) Multi-echo acquisition of MR angiography and venography of the brain at 3 Tesla. JMRI 30:449–454

25. Taber KH, Hayman LA, Herrick RC et al (1996) Importance of clot structure in gradient-echo magnetic resonance imaging of hematoma. J Magn Reson Imaging 6:878–883

26. Cho KH, Kim JS, Kwon SU et al (2005) Significance of susceptibility vessel sign on T2*-weighted gradient echo imaging for identification of stroke subtypes. Stroke 36:2379–2383

27. Shinohara Y, Kinoshita T, Kinoshita F (2012) Changes in susceptibility signs on serial T2*-weighted single-shot echo-planar gradient-echo images in acute embolic infarction: comparison with recanalization status on 3D time-of-flight magnetic resonance angiography. Neuroradiology 54:427–434

28. Liebeskind DS, Sanossian N, Yong WH et al (2011) CT and MRI early vessel signs reflect clot composition in acute stroke. Stroke 42:1237–1243